Technical Report

Pattern Recognition and Image Processing Group
Institute of Computer Aided Automation
Vienna University of Technology
Favoritenstr. 9/1832
A-1040 Vienna AUSTRIA
Phone: +43 (1) 58801-18351
Fax: +43 (1) 58801-18392
E-mail: lettner@prip.tuwien.ac.at
URL: http://www.prip.tuwien.ac.at/

PRIP-TR-89 September 6, 2004

Texture Analysis of Painted Strokes

Martin Lettner, Paul Kammerer and Robert Sablatnig

Abstract

In this practical work texture analysis for painted strokes is reported. The work presents a study of stroke classification in which two classes of strokes are identified: fluid and dry strokes. The discrimination is done with a feature vector which is extracted from the stroke texture by the help of texture analysis methods. To find an adequate texture analysis method for this application, three different texture analysis methods are executed on test images from painted strokes. The methods applied are based on statistical features of first and second order and on the discrete wavelet transformation, whereas the statistical features of second order are extracted from the co-occurrence matrix. The results are compared and it turns out that the wavelet based texture analysis method yields the best discrimination rate for this application.

Contents

1 Introduction **2**

2 An Overview about Texture Analysis **2**
2.1 Statistical Methods 4
2.2 Geometrical Methods 4
2.3 Model Based Methods 5
2.4 Signal Processing Methods 5

3 The Test Panels and the Painted Strokes **6**
3.1 The Drawing Tools and Materials 6
3.2 Texture Attributes of the Strokes 7

4 The Texture Analysis Methods **7**
4.1 Statistical Features of First Order 9
4.2 Gray Tone Spatial Dependence Matrix 10
4.3 The Wavelet Transformation 12
4.3.1 Continuous Wavelet Transformation 12
4.3.2 Discrete Wavelet Transformation 12

5 Experiments **14**
5.1 The Test Images 15
5.2 Results from the Statistical Features of First Order 16
5.3 Results from the Co-Occurrence Matrix 16
5.4 Results from the Discrete Wavelet Transformation 17
5.5 Comparison of the Methods 19
5.6 Rotation Test 22

6 Summary and Conclusion **24**

1 Introduction

The recognition of painted strokes is an important step in analyzing painted works of art like panel paintings, independent drawings and underdrawings. Underdrawings constitutes the basic concept of an artist when he starts the creation of his work of art. They are normally hidden by paint layers in the finished painting. With the help of infrared reflectography it is possible to view through the different paint layers and thus make the underdrawing visible. But even for art experts, it is difficult to recognize all drawing tools and materials used for the creation of the strokes. The use of computer based imaging technologies brings a new and objective analysis method and assists the art expert in analyzing paintings.

Painted strokes or lines can be painted either in dry or fluid drawing materials. Chalk or graphite are examples for dry materials and paint or ink applied by pen or brush are examples for fluid painting materials. Strokes applied with chalk or graphite have different features like boundary characteristics, thickness or texture in comparison to the strokes drawn with pen or brush. To give an example, fluid lines have smooth boundaries and they vary in width and density. Dry materials have less variation in width, they are less continuous and the texture is more granular, irregular, and coarse with a variety of gray levels. Compared to dry materials the texture from liquid painting materials is smooth and homogeneous.

The boundary characteristics of painted strokes have been already used to recognize them [8]. This work deals with the analysis of the stroke texture in order to recognize strokes and their underlying drawing material. The strokes are classified into two classes: one for strokes drawn in dry painting materials and the other for strokes drawn in fluid painting materials. The classification is performed based on features extracted from the texture. To find an adequate and practicable texture analysis method for feature extraction especially for the stroke application three different texture analysis methods are applied and compared for this analysis. The first method is based on statistical features of first order. The second one is based on the co-occurrence matrix and the third method is a signal processing method based on the discrete wavelet transformation. Reasons for deciding these methods are given in Section 4. The strokes for this work are provided on test panels applied by a restorer.

The organization of this document is as follows. In the next section a short overview about texture analysis is given. Section 3 describes the painted strokes used for this work. Section 4 covers the texture analysis methods used. Experimental results are given in Section 5 and finally Section 6 gives a summary and a conclusion.

2 An Overview about Texture Analysis

We recognize texture when we see it but it is difficult to define [20]. Already since the mid seventies some definitions for texture came up. Through the growing number of applications more definitions for texture accrued over the years and got more complex. These applications range from automated inspection problems and the defect detection in images of textiles to remote sensing and the classification of different types of terrains.

An example definition for texture from IEEE Standard Glossary of Image Processing and Pattern Recognition Terminology [21]:

> *Texture is an attribute representing the spatial arrangement of the gray levels of the pixels in a region.*

Another definition from A. K. Jain in Fundamentals of Image Processing [7]:

> *The term texture generally refers to repetition of basic texture elements called texels. The texel contains several pixels, whose placement could be periodic, quasi-periodic or random. Natural textures are generally random, whereas artificial textures are often deterministic or periodic. Texture may be coarse, fine, smooth, granulated, rippled, regular, irregular, or linear.*

There are four major issues in the field of texture analysis [20]:

Texture Segmentation: deals with the partition of a textured image into regions which have homogeneous properties with respect to texture.

Texture Classification: refers to classify a texture into a given number of predefined categories.

Texture Synthesis: the goal is to build a model of image texture, which can then be used for generating the texture.

Shape from Texture: is about the reconstruction of 3D surface geometry from texture information in 2D images.

These four issues require an efficient description of image texture with several features. Texture analysis methods yields a set of textural features for image-texture description. Tuceryan and Jain divided texture analysis methods into four categories [20]:

- Statistical Methods
- Geometrical Methods
- Model Based Methods
- Signal Processing Methods

In the following sections a list of some general methods will be explained. It is only a short survey of some well known methods without emphasizing details. The methods performed in the practical work are described in more detail in Section 4.

2.1 Statistical Methods

Statistical texture analysis methods are based on principles in the distribution of the gray levels from the individual pixels. Depending on the number of pixels defining the features, statistical methods can be further classified into first order (one pixel), second order (two pixel) and higher order (three or more pixel) statistics.
First order statistical methods consider the individual pixel values without a spatial interaction. The methods are very simple and different textures can have the same features. The features calculated can be mean, variance, skewness, kurtosis, energy and entropy [11]. The mean is the average gray level from the image pixels and the variance describes the variation around the mean. The skewness is an indication of symmetry of the histogram and the kurtosis is a measure of flatness. The energy describes the information content in the image and the entropy is a measure of histogram uniformity.
Statistical methods of second order observe the spatial distribution. The spatial distribution is important for defining the quality of texture. Several methods came up in the early seventies of the last century:

Co-Occurrence Matrix The most widely method used in texture analysis is the gray tone spatial dependence matrix (GTSDM). The method was proposed by Haralick, Shanmugan and Dinstein in 1973 [6]. The gray tone spatial dependence matrix also named co-occurrence matrix is a $N \times N$ matrix, which describes the spatial dependency from the gray levels. N is the number of gray levels in the original image. Different statistical features can be calculated from the matrix. Being a famous method in texture analysis and coming off well in several works [5, 19] the method is used in the practical work and thus specified in more detail in Section 5.

Autocorrelation Features The character from a textured image depends on the spatial size of texture primitives. Large texture primitives (texel) build up a coarse texture and in contrast small primitives give up rise to fine texture. Thus the periodicity from the texel builds up an important character in textured images. The autocorrelation coefficient describes the spatial coherence between the texels. If the primitives are periodic, then the autocorrelation increases and decreases periodically with distance. The autocorrelation function can be used to analyze the regularity and coarseness of a textured image [20].

Gray Level Run Length Method The gray level run length method (GLRLM) is based on computing the number of gray level runs of various length. A gray level run is a set of linearly adjacent pixels having the same gray level. The gray level run lengths are computed for four different directions and similar to the GTSDM some features are computed from the resulting matrix.

The performance for texture analysis of autocorrelation features and GLRLM has been found to be relatively poor [5].

2.2 Geometrical Methods

Geometrical methods consider texture to be composed of texture primitives, the texels. The methods try to find a relationship between the primitives, and not between pixels like the statistical methods. For these methods it is necessary to identify the primitives before starting to analyze the spatial distribution. Tucerjan and Jain classified the geometrical methods further in Voronoi tessellation features and structural methods [20]. Since there exist no real texture primitives in the stroke-texture, geometrical methods are not considered further in this work.

2.3 Model Based Methods

Model based texture analysis methods are based on the construction of an image model that can be used not only to describe texture, but also to synthesize it. The model parameters capture the essential qualities of texture perceived.
Pixel based models interpret an image of a collection of pixels, region based models regard an image as a set of sub patterns placed according to given rules. Various types of models can be obtained with different neighborhood systems. Random Field models analyze spatial variations in two dimensions. These models assume that the intensity at each pixel in the image depends on the intensities of the neighboring pixels. A representative method are the Markov Random Fields [11].

2.4 Signal Processing Methods

Signal processing methods analyze the frequency content of the image. Signal processing methods are a very important aspect in texture analysis, because psychophysical research has given evidence that the human brain does a frequency analysis of images [20]. Close to other methods signal processing methods compute certain statistical features, like mean magnitude, from the filtered images to describe the texture.

The Fourier Transformation The Fourier transformation is an analysis of the global frequency content in the signal without any reference to localization in the spatial domain. The Discrete Fourier transformation DFT is the sampled Fourier transformation and therefore does not contain all frequencies forming the image. The number of frequencies corresponds to the number of pixels in the real domain image. For a square image $N \times N$, the two dimensional DFT is given by:

$$F(k,l) = \frac{1}{N^2} \sum_{i=0}^{N-1} \sum_{j=0}^{N-1} f(i,j) e^{-i2\pi(\frac{ki+lj}{N})} \tag{1}$$

where $f(i,j)$ is the image in the real space and the exponential term is the basis function corresponding to each point $F(k,l)$ in the Fourier space. Statistical features are extracted from the Fourier space (spatial domain) to describe the image texture. The results for texture analysis are poor [5].

Short Time Fourier Transformation The Short Time Fourier transformation (STFT) or Windowed Fourier transformation is a similar to the Fourier transformation but the analysis is localized in the spatial domain. This is handled by introducing spatial dependency into the Fourier analysis.

Multiresolution Analysis Many applications require the analysis to be localized in the spatial domain. The wavelet transformation is an improvement of the STFT. A multi resolution analysis (e.g. the wavelet transformation) is achieved by using a window function, which is changed in scale and time. If the window function is Gaussian, the obtained transformation is called the Gabor transformation. Gabor and wavelet transformations are nowadays widespread methods and many researchers use these methods for their work in texture analysis [4, 1, 3, 14, 18]. The wavelet transformation is explained in more detail in Section 4.

3 The Test Panels and the Painted Strokes

The experiments are performed on four different test panels which are created by an art expert. The test panels are digitized using a flat-bed scanner with an optical resolution of 1200 dpi.
The panels are prepared with different groundings and there are several strokes applied with different drawing tools and materials. The first layer is the panel itself. Next, there is a ground layer (a priming) on which the visible stroke (the third layer) is applied. Because of the different grounding on the test panels, the painting materials are accepted differently on the panels and a classification of strokes from different prepared panels was not done in this work. Figure 1 shows panel 1 where the six considered strokes for this work are applied. The order of the strokes from row 1 to 6 on the panel is as follows: graphite, black chalk, brush, quill, reed pen and silver point. More information from the drawing materials and texture information from the strokes is given in the next two sections.

3.1 The Drawing Tools and Materials

The two main groups for the strokes are dry and fluid drawing materials. The following types of strokes are considered for this work: graphite, black chalk and silver point are the representatives for the dry strokes and brush, quill and reed pen are the considered fluid strokes.
Figure 2 shows some details from the strokes considered in this work. The stroke texture from the fluid materials, see Figure 2(c), (d) and (e), is more homogeneous in comparison to the texture from the dry drawing materials in Figure 2(a), (b) and (f) which is rather coarse and rough. The roughness from the texture from the dry drawing materials depends from the groundings of the panels. The more plain the underground the finer is the texture from the dry strokes.
Fluid strokes have a more homogeneous surface and texture for all panels. But some fluid drawing materials are not accepted similar on the different groundings. So there are sometimes discontinuities in the surface from fluid strokes. This condition can be seen in Figure 2(e) where the background interfuses the stroke. More characteristics and differences between fluid and dry strokes can be seen in Table 1.

Figure 1: Panel 1: The order of the strokes from row 1 to 6 is as follows: graphite, black chalk, brush, quill, reed pen and silver point.

3.2 Texture Attributes of the Strokes

Unlike other texture analysis applications (most researchers test their texture analysis algorithms with test images from P. Brodatz, *Textures: A Photographic Album for Artists and Designers*) the stroke test images have no texels. Texels are a coherent set of pixels, which build a small unit due to a definite property. The stroke-texture is very inhomogeneous and irregular for dry strokes and nearby a black matrix for fluid strokes. Figure 3 gives a survey of the typical textures from the different strokes. It can be seen that the texture from the liquid painting materials (b) to (d) is nearby homogeneous and the texture from the chalk stroke (a) is more granular. Image (d) is a section from a stroke painted by a reed pen. Figure 2(e) shows another cutoff from a reed pen. The fluid painting material from this tool is not always applied over the whole painting point because of the hard pen. Sporadic background spots appear in the stroke. A survey over these texture characteristics in the strokes applied is given in Table 2.

4 The Texture Analysis Methods

To get a comparative study and to find a practicable and adequate texture analysis method for the stroke application three different texture analysis methods are performed in this work. The first method is based on statistical features of first order. To get first

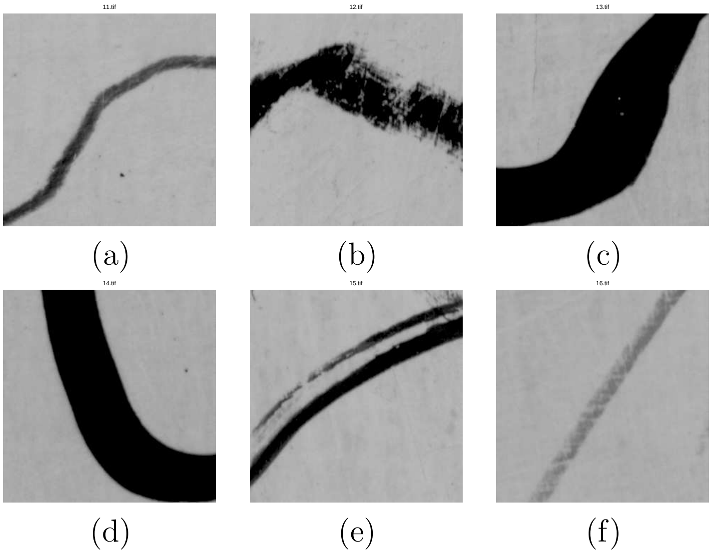

Figure 2: Examples of the strokes on the test panels. (a) is a stroke applied by graphite, (b) shows a black chalk stroke, (c) a brush, (d) quill, (e) reed pen and (f) shows a stroke painted by a silver point.

order statistical features the mean and standard deviation is calculated from the test samples. The second method is based on the co-occurrence method [6] because of its high profile and separate studies have shown that this method outperforms the others in texture discrimination [5, 19]. Conners and Harlow compared the method with run length difference, gray level difference density, and power spectrum [5]. Sharma, Markou and Singh showed that the co-occurrence features yield the best results compared to auto-correlation, edge frequency, primitive-length, and Laws method [19].
Having no typical texel in the stroke texture several geometrical and model based methods are useless. So using a signal processing method in the opposite to the statistical methods above is adequate. The wavelet transformation based texture analysis got the preference for this application because the wavelet decomposition enables a multiresolution analysis,

Fluid lines:
- continuous
- vary in width and density
- pooling of paint at the edges
- droplet at the end

Dry lines:
- less variation in width
- less continuous
- more granular

Table 1: Basic attributes of the different strokes.

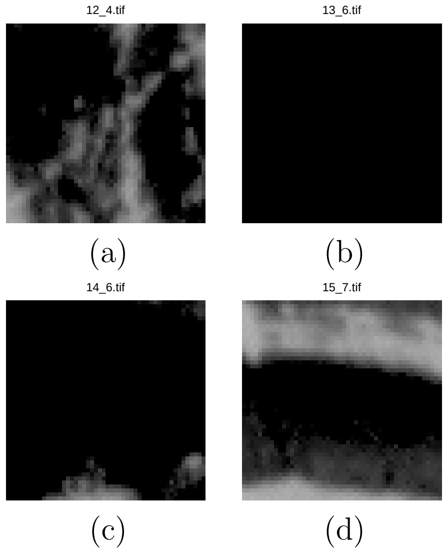

Figure 3: Typical textures from the strokes. (a) shows the texture from a chalk stroke. The texture is very coarse. (b) shows a brush stroke with a homogeneous black matrix. (c) is a quill stroke with a blemish. Such discontinuous parts appear by all strokes, depending from the grounding. (d) finally shows a reed pen stroke where the painting material was not accepted over the whole breadth .The matrix size constitutes 50×50.

this is a time and frequency analysis, and the wavelet transformation showed good results in several studies [16, 2, 17].
In this section the texture analysis methods performed in the work will be explained in more detail. The first subsection describes the statistical features of first order. The second shows the co-occurrence method and the third gives an survey about the wavelet transformation.

4.1 Statistical Features of First Order

Statistical features of first order regard the individual gray values from the pixels in a $n \times m$ matrix $\mathbf{R}$ but the spatial arrangement is not considered, i.e. different textures can have the same gray level histogram.
To get an feature vector with statistical features of first order the mean and standard deviation were calculated from the test samples. Equations 2 and 3 show the mean $\bar{x}$ and the standard deviation s from a matrix $\mathbf{R}$:

$$\bar{x} = \frac{1}{mn} \sum_{i=0}^{n} \sum_{j=0}^{m} \mathbf{R}(i,j) \ , \tag{2}$$

$$s = \sqrt{\frac{1}{mn} \sum_{i=0}^{n} \sum_{j=0}^{m} (\mathbf{R}(i,j) - \bar{x})^2} \ . \tag{3}$$

Graphite: A stroke applied by a graphite pencil is very narrow. Test samples have a size from maximal 25×25.

Black Chalk: A chalk stroke has a very rough and coarse texture. The boundaries vary unlike the other dry strokes in width. Unlike the fluid strokes, the pixels have many different gray levels.

Brush: A fluid stroke applied by brush, has a nearby homogeneous black texture. Starting Point and endpoint differ in width to the centerpiece of the stroke.

Quill: The quill makes also strokes with a homogeneous black texture, the width is nearby constant.

Reed Pen: The reed pen strokes are also very similar to the two other fluid strokes. But strokes applied by a reed pen have some irregularities in the surface.

Silver Point: Silver point strokes look pale and the width is narrow like the graphite strokes.

Table 2: Texture attributes of the different strokes. Examples for the strokes are given in Figure 2.

4.2 Gray Tone Spatial Dependence Matrix

The GTSDM or often termed as co-occurrence matrix is a very popular tool for texture analysis. It has been presented in 1973 by Haralick, Shanmugam and Dinstein [6]. The $N \times N$ co-occurrence matrix describes the spatial alignment and the spatial dependency of the different gray levels, whereas N is the number of gray levels in the original image. The co-occurrence matrix $P_{\phi,d}(i,j)$ is defined as follows. The entry (i,j) of $P_{\phi,d}$ is the number of occurrences of the pair of gray levels i and j at inter-pixel distance d and the direction angle ϕ. The considered direction angles are 0°, 45°, 90° and 135°. Note that the matrices are symmetric: $P_{\phi,d}(i,j) = P_{\phi,d}(j,i)$.
To explain the method, a short example shows the problem. Consider Figure 4 (a) which represents a 4×4 matrix $\mathbf{I}$. The matrix represents an image with four gray tones, ranging from 0 to 3. Figure 4 (b) to (e) shows the calculated spatial gray level dependence matrices with $d = 1$ and the four direction angles $\phi = \{0°, 45°, 90°, 135°\}$. The elements (i,j) in the four calculated co-occurrence matrices $P_{\phi,d}$ indicate the number of occurrences of the pair of gray levels i and j in the respective angle ϕ at distance $d = 1$. For instance, the element in the position $(i,j) = (2,2)$ of the distance 1 horizontal $P_{0°,1}$ matrix is the total number of times two gray tones of value 2 occurred horizontally adjacent to each other. There are three in 0° direction and because of the symmetric character three in 180° direction. This results to 6 occurrences of gray tones 2 in the matrix $P_{0°,1}$ at position $(2,2)$.
To describe a texture with a plenty of co-occurrence matrices is much to circuitous because of waisting place. It has no sense to calculate co-occurrence matrices for a few distance

$$\mathbf{I} = \begin{pmatrix} 0 & 0 & 1 & 1 \\ 0 & 0 & 1 & 1 \\ 0 & 2 & 2 & 2 \\ 2 & 2 & 3 & 3 \end{pmatrix}$$
(a)

$$P_{0^\circ,1} = \begin{pmatrix} 4 & 2 & 1 & 0 \\ 2 & 4 & 0 & 0 \\ 1 & 0 & 6 & 1 \\ 0 & 0 & 1 & 2 \end{pmatrix}$$
(b)

$$P_{90^\circ,1} = \begin{pmatrix} 6 & 0 & 2 & 0 \\ 0 & 4 & 2 & 0 \\ 2 & 2 & 2 & 2 \\ 0 & 0 & 2 & 0 \end{pmatrix}$$
(c)

$$P_{135^\circ,1} = \begin{pmatrix} 2 & 1 & 3 & 0 \\ 1 & 2 & 1 & 0 \\ 3 & 1 & 2 & 0 \\ 0 & 0 & 2 & 0 \end{pmatrix}$$
(d)

$$P_{45^\circ,1} = \begin{pmatrix} 4 & 1 & 0 & 0 \\ 1 & 2 & 2 & 0 \\ 0 & 2 & 4 & 1 \\ 0 & 0 & 1 & 0 \end{pmatrix}$$
(e)

Figure 4: (a) 4×4 image with four gray levels. (b)-(e) shows the calculation of the co-occurrence matrix with $d = 1$ and $\phi = \{0°, 45°, 90°, 135°\}$.

and direction parameters d and ϕ. Hence Haralick suggested 14 features which can be worked out from the co-occurrence matrix. These features build up an feature vector with which the description and classification from textured images is done. For this work four popular features were used. These features are the energy, inertia, entropy and the homogeneity. Table 3 shows the equations for these features whereas N denotes the size from the co-occurrence matrix $P_{\phi,d}$.

Energy:

$$E = \sum_{i=1}^{N-1} \sum_{i=1}^{N-1} P_{\phi,d}^2(i,j) \tag{4}$$

Inertia:

$$I = \sum_{i=1}^{N-1} \sum_{i=1}^{N-1} (i-j)^2 P_{\phi,d}(i,j) \tag{5}$$

Entropy:

$$H = \sum_{i=1}^{N-1} \sum_{i=1}^{N-1} P_{\phi,d}(i,j) log P_{\phi,d}(i,j) \tag{6}$$

Homogeneity:

$$L = \sum_{i=1}^{N-1} \sum_{i=1}^{N-1} \frac{1}{1+(i-j)^2} P_{\phi,d}(i,j) \tag{7}$$

Table 3: The equations for features calculated from the co-occurrence matrix.

4.3 The Wavelet Transformation

Multiresolution techniques tend to transformation images into a representation in which both spatial and frequency information is present. The wavelet paradigm is well established and it is a modern and popular tool for texture analysis. In the past times it has been successfully used [14, 15, 3, 2, 9, 17, 1, 13]. Basics in wavelet transformation will be explained in this section.

4.3.1 Continuous Wavelet Transformation

The wavelet decomposition of a signal $f(t) \in \mathbf{L}^2(\mathbf{R})$ is performed by a convolution of the signal $f(t)$ with a family of real orthonormal bases $\psi_{a,b}(t)$ obtained through translation and dilation of a kernel function $\psi(t) \in \mathbf{L}^2(\mathbf{R})$ known as the mother wavelet, i.e.,

$$\psi_{a,b}(t) = \frac{1}{\sqrt{|a|}}\psi\left(\frac{t-b}{a}\right). \tag{8}$$

where $a, b \in \mathbf{R}$ $(a \neq 0)$ are referred to as the dilation and translation parameters, respectively. The continuous wavelet transformation of a function $f(t) \in \mathbf{L}^2(\mathbf{R})$ is defined as

$$c_f(a,b) = \int\limits_{-\infty}^{+\infty} \psi^*_{a,b}(t) f(t) \mathrm{d}t = \langle \psi_{a,b}(t), f(t) \rangle. \tag{9}$$

The continuous wavelet transformation CWT is the sum over all time of the signal multiplied by scaled and shifted versions of the wavelet function ψ. The function $f(t)$ can be recovered from its transformation by the following reconstruction formula:

$$f(t) = \frac{1}{C_\psi} \int\limits_{-\infty}^{+\infty} \int\limits_{-\infty}^{+\infty} c_f(a,b)\psi_{a,b}(t) \frac{\mathrm{d}a\,\mathrm{d}b}{a^2}. \tag{10}$$

The extension to the 2D case is usually performed by using a combination of 1D transforms.
Continuous shifting and scaling from the wavelet function $\psi_{a,b}$ over the signal $f(t)$ and calculating the correlation between the original signal $f(t)$ and the scaled and shifted versions of the wavelets $\psi_{a,b}$ produces a lot of data, the wavelet coefficients $c_{a,b}$, which is highly redundant. It turns out that scales and positions based on powers of two will be much more efficient [12].

4.3.2 Discrete Wavelet Transformation

The discrete wavelet transformation DWT is a subset of scale and space coefficients from the CWT. The DWT [10],[1] decomposes an original signal $f(x)$ with a family of basis functions $\psi_{m,n}(x)$, which are dilations and translations of a single prototype wavelet function known as the mother wavelet $\psi(x)$:

$$f(x) = \sum_{n=0}^{\infty}\sum_{n=0}^{\infty} c_{m,n}\psi_{m,n}(x) \ . \tag{11}$$

Equation 8 can be discretized by restraining a and b to a discrete lattice $a = 2^m, b = n \in \mathbf{Z}$ [18]. m and n scale and dilate the mother function $\psi(x)$ to generate wavelets:

$$\psi_{m,n}(x) = 2^{-m/2}\psi(2^{-m}x - n). \tag{12}$$

The scale index m indicates the wavelet's width, and the location index n gives the position. The discrete wavelet transformation coefficients $c_{m,n}$ can be calculated by the inner products $\langle \psi_{m,n}(x), f(x) \rangle$ which are the estimation of signal components centered at $(2^{-m}n, 2^m)$ in the time frequency plane [3].
An efficient way to implement this scheme using filters was developed by Mallat [10]. The 2D DWT is computed by a pyramid transform scheme using filter banks. The filter banks are composed of a low pass and a high pass filter and each filter bank is then sampled down at a half rate of the previous frequency. The input image is convolved by a high pass filter and a low pass filter in horizontal direction (rows). After this step another convolution in vertical direction (columns) is performed with a high and a low pass filter. Figure 5 shows this procedure. The input image cA_0 is convolved by a high pass filter Hi_D and a low pass filter Lo_D in horizontal direction. After this step another convolution in vertical direction is performed. By repeating this procedure it is possible to obtain wavelet decomposition of any order. According to this procedure, the original

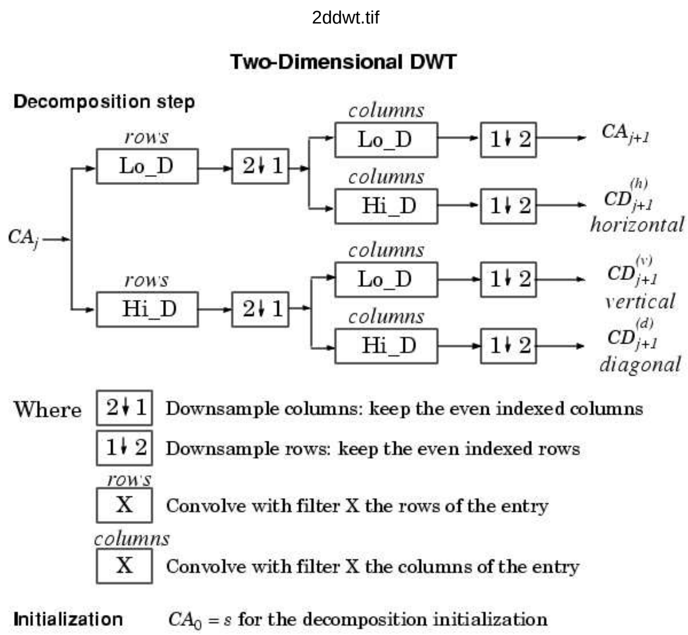

Figure 5: The 2 dimensional discrete wavelet transformation [12].

image can be transformed into four subimages [3], namely

- LL subimage: Horizontal and vertical directions have low frequencies. The corresponding subimage is an approximation of the input image.

- LH subimage: The horizontal has low frequencies and the vertical one has high frequencies.
- HL subimage: The horizontal direction has high frequencies and the vertical one has low frequencies.
- HH subimage: The horizontal and vertical directions have high frequencies.

According to Figure 5 the subimage cA corresponds to the LL subimage, $cD^{(h)}$ to LH, $cD^{(v)}$ to HL and $cD^{(d)}$ to the HH subimage.
Smooth images and textures have strong components in the low frequencies and textured images in which the gray levels varies rapidly have substantial components in a wide frequency/scale spectrum. Smooth and textured images can thus easily be distinguished by examining their wavelet transformation.
A three level decomposition results in 10 sub images, see Figure 6(a) whereas the approximation image is the input image for the next level. Statistical information calculated from the resulting channels can be used as the texture features. Here the mean of the coefficient magnitudes is used to build up the feature vector:

$$e_n = \frac{1}{MN} \sum_{i=1}^{M} \sum_{j=1}^{N} |c(i,j)| \ . \tag{13}$$

where the channel is of dimension $M \times N$, c is a wavelet coefficient within the channel and n denotes the channel number. The calculation of the energy for each channel results in 10 features per image. Images in which the gray levels vary smoothly are heavily dominated by the low-frequency channels in their wavelet transform. Textured images have large energies in the low and middle frequencies.
The proposed scheme from Porter [14] did not achieve rotation invariance. Therefore Porter proposed an extended and improved algorithm to achieve rotation invariance by combining pairs of diagonally opposite wavelet channels to form single features [15]. The LH and HL subimage after each decomposition step are grouped together to produce four main frequency bands as illustrated in Figure 6 (b). The HH channels are not used as they tend to contain the majority of noise. The energy levels in each of the four chosen bands are calculated to create a four dimensional feature vector which is then used for texture classification.

5 Experiments

The classification of the feature vectors was done using the k-means clustering algorithm. This clustering technique has been already applied in several works in texture analysis [14, 4]. The number of clusters constitutes 2: one for dry and and one for fluid strokes.
The experiments were executed with images of matrix sizes 20×20, 25×25, 32×32 and 50×50 with 50 test samples per panel and matrix size. A problem is the tiny width of some strokes (silver point and graphite). 32×32 and 50×50 matrices which do not only cover the whole stroke but also background are not considered. Thus only small matrix sizes are possible for the analysis and this limits the classification rate because texture

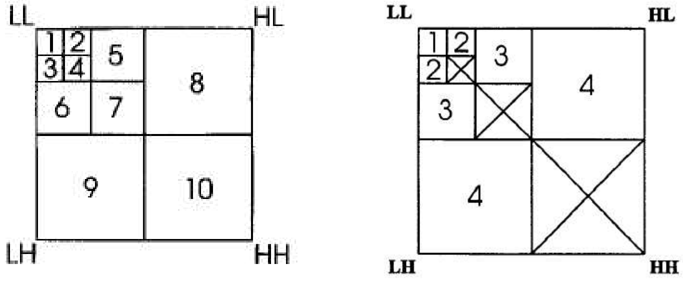

(a) (b)

Figure 6: (a) 10 channels of a three level wavelet decomposition of an image. (b) Grouping of wavelet channels to form 4 bands to calculate the features.

information is lost by decreasing the matrix size. Haralick [6] used a size from 64×64 for his experiments. But for the stroke application this size is too big. Thus the first experiment was done by 50×50 matrices although the graphite stroke at all and the reed pen stroke from Panel 3 and 4 could not be discarded because these strokes are to fine. The next matrix size for the test images constitutes 32×32, but the graphite stroke is still too wide. Further experiments were carried out with an matrix size from 20×20 and 25×25.
The results from the executed experiments with the generated test samples are shown in this section. At first the experimental setup is illustrated, then the individual results from the methods preformed are given (illustrated with the results from panel 1) and then a comparison between the methods and the matrix sizes is given. Furthermore a rotation test to verify the rotation dependency has been carried out and the results are shown at the end of this section.

5.1 The Test Images

To test the different methods for this application, 200 test images in the size of 20×20 and 25×25 have been generated from the four scanned panels. To find the optimal matrix size for the methods, furthermore 320 test images in the size of 32×32, and 160 test images in the size of 50×50 have been generated. With the 50×50 and 32×32 matrices the graphite and silver point have not been considered because of their narrow width. A 50×50 or 32×32 matrix covers not only the stroke but also the background. This results in overall 880 test images of different size. Figure 3 shows examples for 50×50 test images.
The naming convention of the test images is as follows: the first digit in the name is the panel number ranging from 1 to 4. The second digit gives the different strokes, where 1 stands for a graphite stroke, 2 is a black chalk stroke, 3 a brush stroke, 4 is a quill stroke, 5 reed pen and 6 is a silver point stroke. The digit after the underline from 0 to 9 is an test image from the assigned stroke before. This naming convention is for all tests the same and the name can be seen in some diagrams in this document.

5.2 Results from the Statistical Features of First Order

For the first part of the work the Matlab commands `mean2` and `std2` were executed on the test images to simply get a two dimensional feature vector with statistical features of first order. Figure 7 gives an survey about the results of the first attempt in this work. It shows the results (`mean2` and `std2`) from the 50×50 test images from Panel 1. As expected the black chalk strokes (`12_0.tif` to `12_9.tif`) have higher mean values because the texture is not homogeneous black and pixels with brighter gray values are present in the texture. The standard deviation for the black chalk shows also high values because of the roughness of the texture. But also some reed pen strokes show high mean and standard deviation values because of the failures in the surface where the painting material on the panels is not accepted over the whole stroke breadth. After clustering these results with the k-means algorithm, six from forty test images were classified wrong.

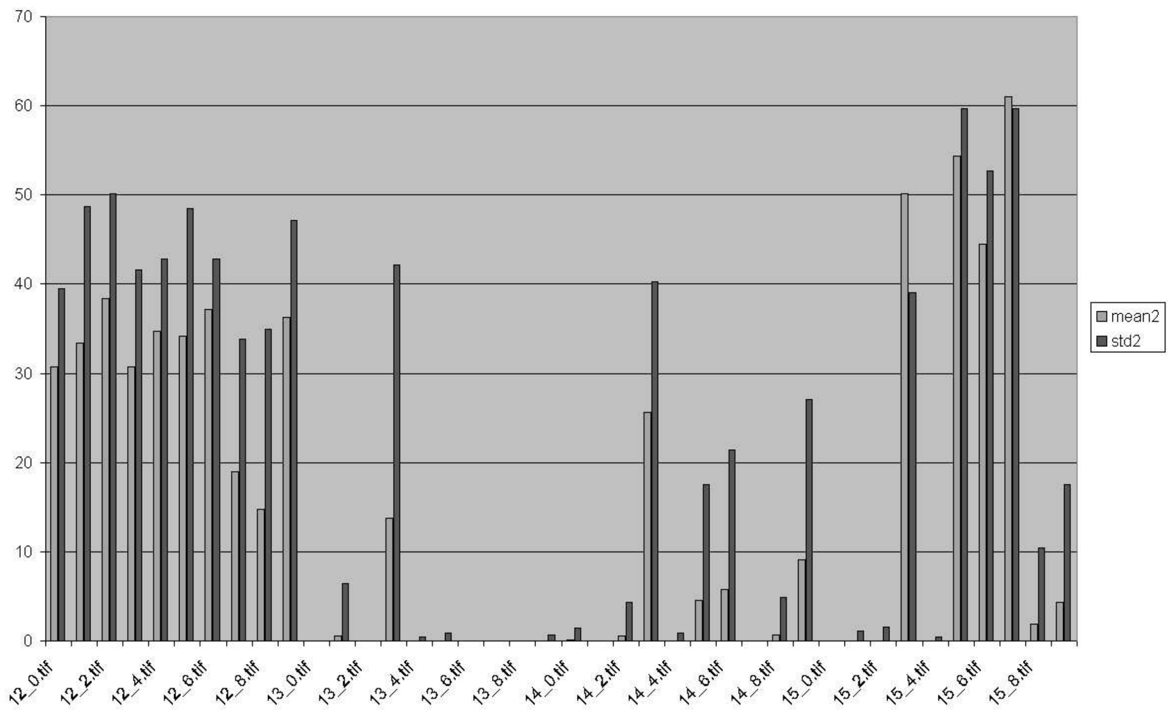

Figure 7: Results from the features from the statistical texture analysis of first order.

5.3 Results from the Co-Occurrence Matrix

Calculating the co-occurrence matrix and the features was done with a Matlab script. The regarded distance for calculating the co-occurrence matrices constitutes $d = 1$ and having no definite direction in the texture the four possible direction angels are sum up. As a result of the 256 gray levels in the test images the co-occurrence matrices have a size

of 256×256.
Figure 8 shows the resulting co-occurrence matrices for the images shown in Figure 3. The information in the matrices concentrates at the diagonal of the matrix. It indicates that the texture changes smoothly throughout the image. The homogeneous matrix for the brush stroke, see Figure 3(b) has a homogeneous black co-occurrence matrix, except the element $P_{\phi,1}(0,0)$ due to the fact that there are only black to black (0 to 0) transitions in the test image.

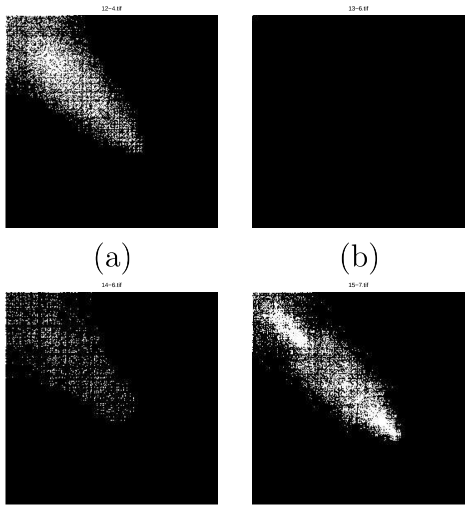

(a) (b) (c) (d)

Figure 8: The co-occurrence matrices for the texture test images in Figure 3.(a) shows the image from the co-occurrence matrix from a chalk stroke, (b) from the brush stroke, (c) from the quill stroke and (d) shows the co-occurrence matrix for the reed pen stroke.

Figure 9 shows the features calculated for the 40 50×50 test images from panel 1. The energy and homogeneity has high values for the fluid strokes because of their homogeneous black texture. The inertia shows a very good result to differentiate between fluid and dry materials. After clustering the 4 features with the k-means algorithm into 2 cluster (dry and fluid) only 3 test images were classified wrong. As can be seen in the diagrams in Figure 9 it is not possible to distinguish between different fluid strokes (`13_0.tif` to `15_9.tif`)
Smaller matrices than the 50×50 showed worse results because texture information gets lost by decreasing the matrix size. Only the results from panel 1 with the 32×32 matrices show feasible results. The results for panel 3 and 4 show a low percentage of correct classification from only 60 to 80 percent. The grounding on these two panels accepts the fluid painting materials inferior than the grounding preparation from panel 1 and 2.

5.4 Results from the Discrete Wavelet Transformation

The discrete wavelet decomposition for the test images was calculated with the help of the Matlab's Wavelet Toolbox. Figure 10 and 11 show the subimages from the three

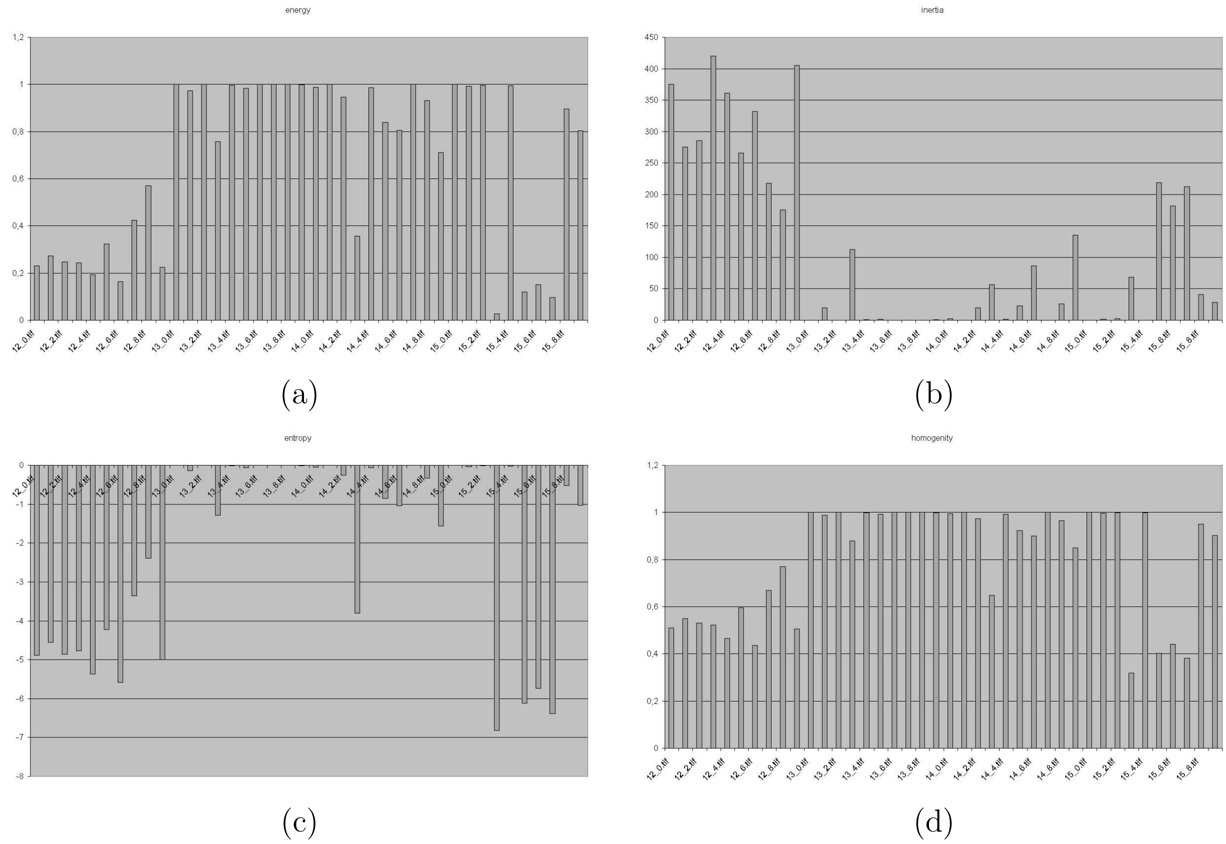

Figure 9: Diagrams for the results from the features from the co-occurrence matrix. (a) shows the energy calculated for the 40 test images from panel 1. (b) shows the inertia, (c) the entropy and (d) shows the homogeneity.

level wavelet decomposition from the strokes in Figure 3 (a) and (c). Remember that the subimages have less pixels as the image of the level above. It can be seen that the subimages from the black chalk stroke in Figure 10 have higher frequency parts in all subimages. The approximation image $A3$ from the quill stroke in Figure 11 has only a few pixels with coefficients unequal to zero, i.e. there are less and lower frequency components.
The best classification results were obtained with an orthogonal and compactly supported wavelet, the Daubechi $db6$ motherwavelet. For a 3 level wavelet decomposition the features for the 10 resulting channels (compare to Figure 6 (a)) were calculated. A four dimensional feature vector with combined channels [15] was also worked out. Figure 12 shows the energies for the strokes shown in Figure 10 and 11. Figure 12(a) shows all 10 features and (b) shows 4 features where the diagonal opposite channels LH and HL were combined and the HH channel is not used. The solid line shows the chalk stroke which has definitely higher frequency components in the low frequency channels. The dotted line shows the energy for the quill stroke which has lower frequency components in all channels.
Better classification results were obtained with the second method. Figure 13 shows the results for the 4 features from the Porter 97 algorithm for all 40 test images from panel

1. As expected the textured images have higher energies in all channels. With the chosen parameters 5 from 40 test images were classified wrong after clustering with the k-means algorithm. This is an accuracy of 87,5 percent.
A difference between the chalk strokes and the reed pen strokes is that the reed pen strokes have higher energies in the first two channels but less energies in the channel number 3 and 4 unlike the chalk stroke, see Figure 13. Thus finding better features from the subimages of the wavelet transformation will produce better results.
The classification from extracted features from smaller matrices showed good results for the wavelet based texture analysis method. The best results are obtained from test images with a size of 32×32 where the accuracy lies within 85 to 100 percent for the images from the 4 panels.

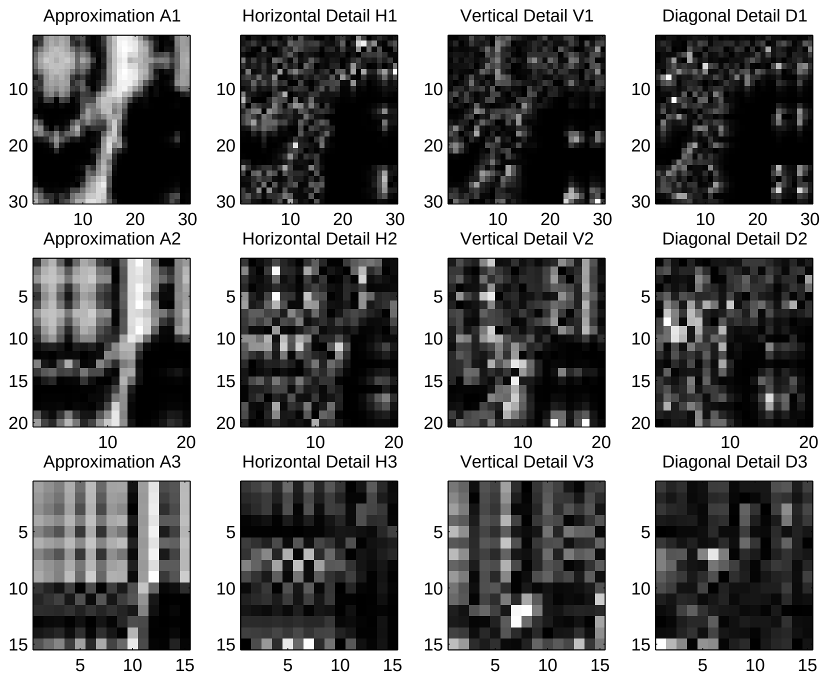

Figure 10: The subimages after wavelet decomposition for the chalk stroke in Figure 3 (a).

5.5 Comparison of the Methods

Table 4 shows the percentage of correct classification for the individual strokes after division into two classes: one for dry strokes (graphite and black chalk) and one for fluid strokes (brush, quill and reed pen). The results are given for all matrix sizes from panel 2 for the three methods performed.
The recognition of the black chalk and the brush stroke showed the best results because the texture is homogeneous over the whole stroke surface. In contrast the texture from the quill and reed pen stroke shows several discontinuities in the surface and thus limits the classification. There are only results for the graphite stroke with matrix size 20×20 and 25×25 because of the tiny width (bigger matrices are marked by an x in the table). The recognition of this type of stroke is good but the classification is bad for the wavelet

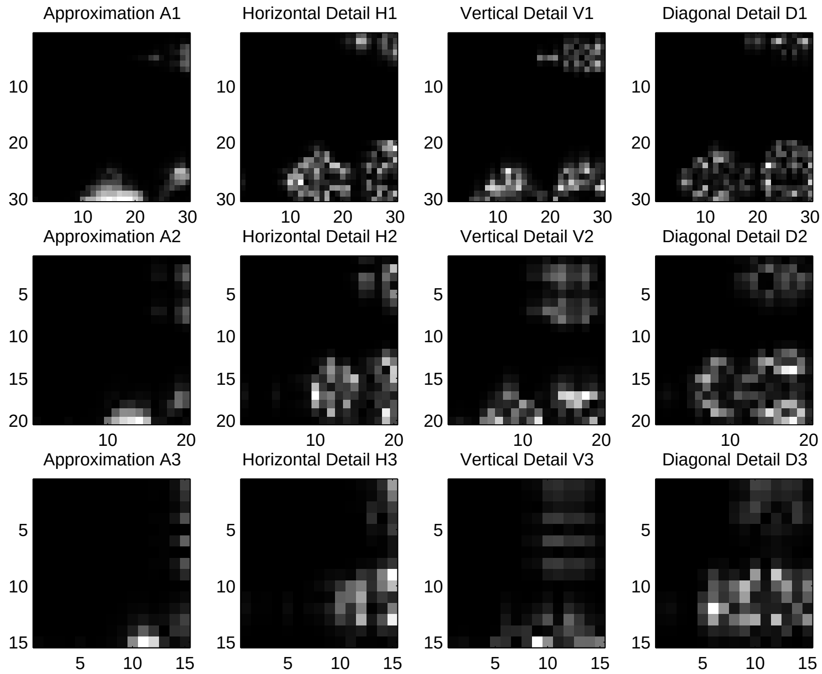

Figure 11: The subimages after wavelet decomposition for the quill stroke in Figure 3 (c).

based features from the 25 × 25 matrices where all graphite strokes are classified as fluid strokes. This classification error rules from the k-means algorithm.
Generally the percentage of correct classification is better for greater matrices but the matrix size is limited by the width from the strokes. The mean value from the three methods for a matrix ranges from 81,3% for the 20 × 20 matrices to 90% for the 32 × 32 matrices. This mean value is annoted in the last column of Table 4.
The results from the different methods are as follows: the best results were obtained with the features from the DWT (using a Daubechies (6) mother wavelet). The classification rate of the statistical features of first order was almost as high as the DWT features but for small matrices the features from the DWT showed better results. The co-occurrence method only performed well for large matrices, but the results are not constant for all four panels. Table 5 shows the results for the different methods compared with the matrix

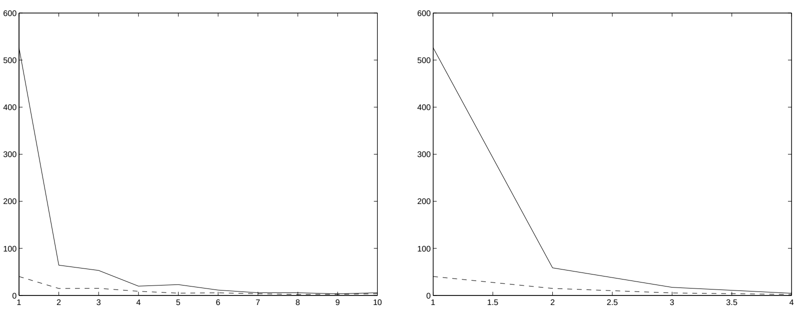

(a) (b)

Figure 12: (a) The energies in the 10 channels for the chalk stroke (solid line) and the smoother quill stroke(dotted line) (b) shows the 4 features for the combined channels.

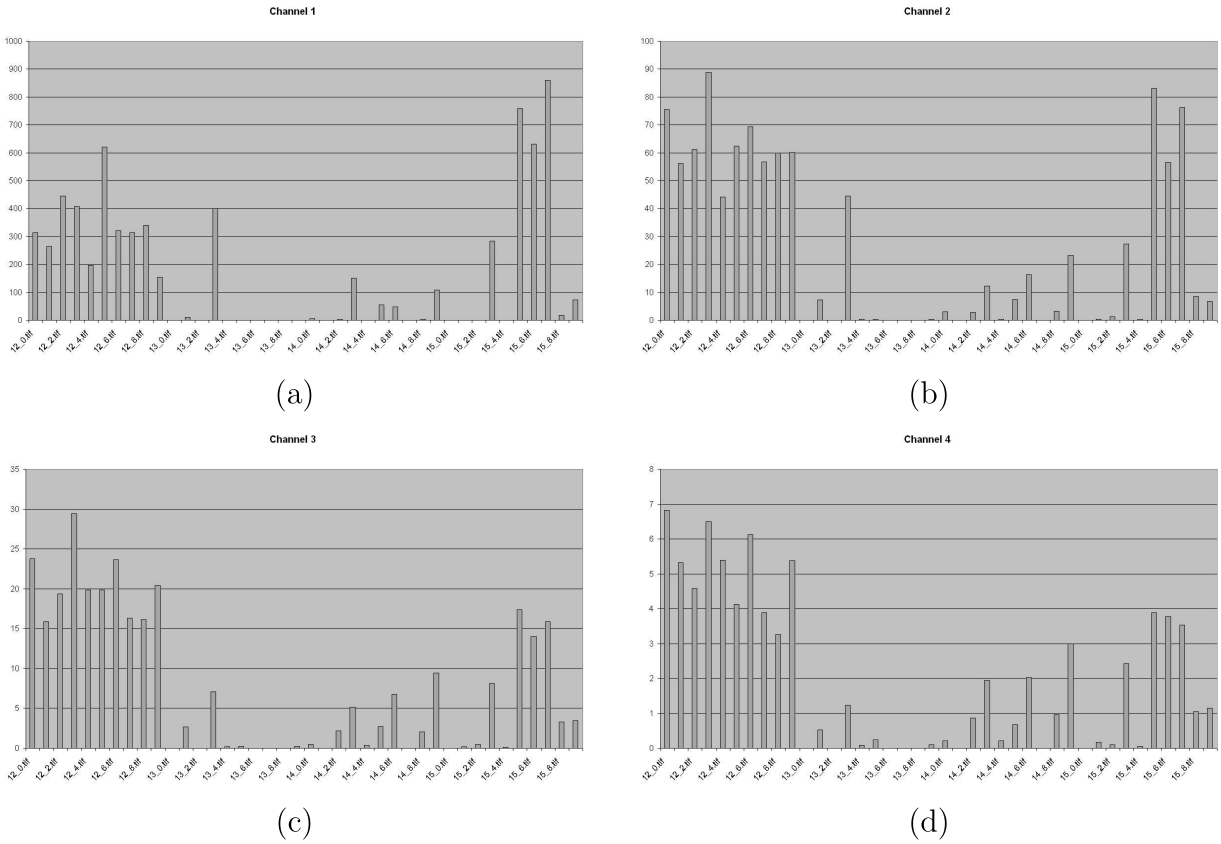

Figure 13: Diagrams for the results for the energy in the four channels.

size for all four panels.
Figure 14 shows the percentage of correct classification using the statistical features of first order, the co-occurrence features and the features from the DWT for all matrix sizes and panels. The horizontal axis shows the different matrix sizes 20×20, 25×25, 32×32 and 50×50 for the four panels (indicated in brackets) and the y-axis shows the percentage of correctly classified strokes. It can be seen that the results are better for large matrix sizes. However the DWT features (the dark gray line with squares) show a good discrimination rate even for small matrices. It turns out that the best classification rate was obtained with the feature vector from the DWT (using the Daubechies (6) mother wavelet) and the matrix sizes 32×32 and 50×50. The break-in by the 25×25 matrices rules from the classification (graphite strokes are allocated to the class of fluid strokes). The classification rate of the statistical features of first order was almost as high as the DWT features for large matrices. The co-occurrence method only performed well for large matrices, but the results are not constant for all four panels.
Finally, Table 6 shows the mean percentage of correct classification over the four panels. The last row shows the mean over the panels and the matrix sizes. The mean percentage of classification constitutes 86,6% for the DWT features, 82% for the statistical features of first order and 74,5% for the features calculated from the co-occurrence matrix.

	Graphite	Bl. Chalk	Brush	Quill	Reed Pen	Total	Mean
20×20							
Statistical features	100	10	70	60	100	68	
Co-occurrence features	50	100	90	100	60	80	
Wavelet based features	100	100	100	100	80	96	81,3
25×25							
Statistical features	100	10	60	40	100	62	
Co-occurrence features	100	100	90	20	30	68	
Wavelet based features	0	100	100	70	60	66	65,3
32×32, 1. Attempt							
Statistical features	x	100	100	100	70	92,5	
Co-occurrence features	x	100	100	90	60	87,5	
Wavelet based features	x	100	100	100	60	90	90
32×32, 2. Attempt							
Statistical features	x	100	100	80	90	92,5	
Co-occurrence features	x	100	100	80	40	80	
Wavelet based features	x	100	100	90	100	97,5	90
50×50							
Statistical features	x	100	100	60	80	85	
Co-occurrence features	x	100	100	60	80	85	
Wavelet based features	x	60	100	70	80	77,5	82,8

Table 4: Percentage of correct classification for the individual strokes from panel 2 after division into two classes: one for dry and one for fluid strokes. The results are shown for the three methods performed and all matrix sizes. Column *Total* shows the percentage of correct classification for the individual methods and column *Mean* shows the mean value from the three individual methods for the individual matrix size.

5.6 Rotation Test

To test the rotation invariance for the three texture analysis methods performed a typical section from a chalk stroke was taken and has been rotated by an angle of 15° for 24 times. After each rotation a 50×50 matrix was taken from the center. The matrices from the rotated images contains similarly the same values, only the peripheral zone differ because of the rotation. For the resulting 24 test images with a size of 50×50 pixels the same algorithms as before has been performed.

The results for the statistical features of first order did not show surprising effects. The mean gray level $\bar{\mathbf{x}}$ from the 24 mean gray values from the test matrices constitutes 47.0314. The standard deviation has a value from $\mathbf{s} = 2.748$. That is a deviation from $5,8\%$. The little value for the standard deviation shows that the entries in the 24 matrices are approximately the same. Only the peripheral zone differs.

To achieve rotation invariance the results for the 24 rotated images for the extracted features from the co-occurrence matrix and the energies in the different channels from the wavelet decomposition have to be approximately the same. The energy, inertia, entropy

	20×20	25×25	32×32	32×32	50×50
Panel 1					
Statistical features	58	68	85	85	85
Co-occurrence features	82	76	92,5	90	92,5
Wavelet based features	72	74	85	85	87,5
Panel 2					
Statistical features	68	62	92,5	92,5	85
Co-occurrence features	80	68	87,5	80	85
Wavelet based features	96	66	90	97,5	77,5
Panel 3					
Statistical features	72	70	100	95	96,7
Co-occurrence features	54	54	80	62,5	70
Wavelet based features	92	68	100	97,5	96,7
Panel 4					
Statistical features	74	64	95	95	96,7
Co-occurrence features	72	62	57,5	57,5	86,7
Wavelet based features	96	64	97,5	92,5	96,7

Table 5: Classification results after division into dry and fluid strokes: comparison of the matrix size.

and the homogeneity from the resulting co-occurrence matrices $P_{\phi,d}$ were calculated for the 24 images. Table 7 shows the mean and the standard deviation for these four features from the 24 matrices. The parameters for the co-occurrence matrix $P_{\phi,d}$ are again a distance $d = 1$ and the results from the four directions were added. The energy has very big deviations, the deviation constitutes over 20 percent from the mean value. The values for inertia, entropy and homogeneity show better results.
The outcomes present that the chosen parameter ($d = 1$) show the best results for the co-occurrence method. For a distance $d = 1$, the mean standard deviation $\bar{\mathbf{s}}$ for the 4 features showed the minimum value of $\bar{\mathbf{s}} = 9.197$. Greater distance values d showed bigger values for the standard deviation. For instance the parameter $d = 2$ shows a mean

	Statistical features	Co-occurrence features	Wavelet based features
20×20	68	72	89
25×25	66	65	68
32×32	93,1	79,4	93,1
32×32	91,9	72,5	93,1
50×50	90,9	83,6	89,6
mean	82	74,5	86,6

Table 6: Classification results: comparison between the methods. The values constitutes the mean percentage of correct classification over the four panels. The last row shows the mean over the panels and the matrix sizes.

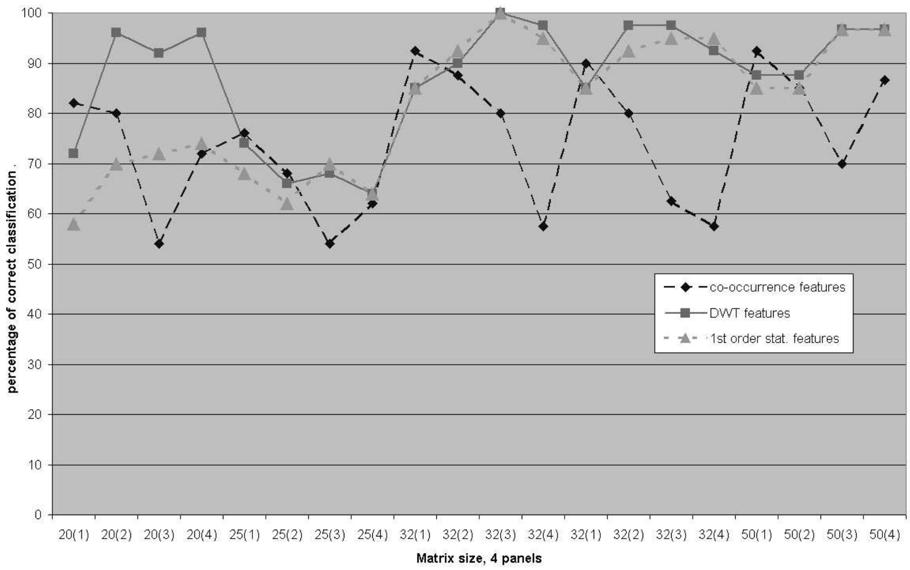

Figure 14: Comparison of experimental results using statistical features of first order, co-occurrence features, and DWT features.

standard deviation from $\bar{\mathbf{s}} = 20,45$.

	Mean	Std. Deviation
Energy	0.0441	0.0097
Inertia	431.0332	44.6033
Entropy	-7.1819	0.1651
Homogeneity	0.2648	0.0181

Table 7: Mean and standard deviation from the 24 matrices for the co-occurrence method.

The rotation test for the features from the wavelet decomposition shows similar results. Table 8 shows the results for this test. Here the standard deviation in the first channel is over 25% from the mean value. The percentage deviation in the other three channels is about 10%.

6 Summary and Conclusion

The work presented has focused on the identification of different stroke textures which are significant for the recognition of the underlying drawing material. The goal of this practical work was to analyze the texture of some test samples from painted strokes to recognize the underlying drawing tool and material. It has been shown that a distinction between fluid and dry materials is possible because the varieties are big enough to distinguish between these two classes. A discrimination between several fluid or dry strokes with

	Mean	Std. Deviation
Channel 1	417.678	110.124
Channel 2	86.260	10.457
Channel 3	27.897	2.660
Channel 4	5.355	0.653

Table 8: Mean and standard deviation from the 24 matrices for the DWT.

texture is not possible because the varieties are to similar. Other features like boundary characteristics have to be added to the feature vector to allow a more precise distinction. From the three texture analysis methods performed, statistical features of first order, co-occurrence method and a wavelet based method, the wavelet based texture analysis method showed the best results. The discrimination with statistical features of first order showed similar results for large matrices (32×32 and 50×50). The co-occurrence method showed also good results for the 50×50 and 32×32 matrices but this matrix size is too big for some strokes (graphite and silver pencil) because of their tiny width.
Better results can be obtained with a variable matrix size which contains enough texture information. A further advancement are better features extracted from the wavelet decomposition. For instance a scheme of improvement for the wavelet based texture analysis method is a fusion of wavelet filters and co-occurrence features, like Clausi and Deng proposed in their paper with Gabor filters [4]. Another alternative to reach better results is to consider the border regions of the strokes, because the biggest variations lies within the border region of the strokes. A method which considers only the relevant pixels in a matrix for the texture analysis is helpful: Pixels belonging to the background are present in the matrix but they do not contribute the features calculated.

References

[1] T. Chang and C.-C.J. Kuo. A Wavelet Transform Approach to Texture Analysis. In *International Conference on Acoustics, Speech, and Signal Processing*, volume 4, pages 661–664. IEEE, March 1993.

[2] T. Chang and C.-C.J. Kuo. Texture Analysis and Classification with Tree-Structured Wavelet Transform. *IEEE Trans. Image Processing*, 2(4):429–441, October 1993.

[3] W. Chumsamrong, P. Thitimajshima, and Y. Rangsanseri. Wavelet-Based Texture Analysis for SAR Image Classification. In *International Geoscience and Remote Sensing Symposium*, volume 3, pages 1564–1566, June 1999.

[4] D.A. Clausi and H. Deng. Fusion of Gabor Filters and Co-occurrence Probability Features for Texture Recognition. In *16th International Conference on Vision Interface*, pages 237–242, Halifax, NS, Canada, June 2003.

[5] R.W. Conners and C.A. Harlow. A Theoretical Comparison of Texture Algorithms. *IEEE Trans. Pattern Analysis and Machine Intelligence*, 2(3):204–222, May 1980.

[6] Robert M. Haralick, K. Shanmugan, and I. Dinstein. Textural Features for Image Classification. *IEEE Trans. System Man Cybernetics*, 3(6):610–621, November 1973.

[7] A. K. Jain. *Fundamentals of Digital Image Processing.* Prentice-Hall, New Jersey, 1989.

[8] P. Kammerer, G. Langs, R. Sablatnig, and E. Zolda. Stroke Segmentation in Infrared Reflectograms. In *13'th Scandinavian Conference, SCIA 2003*, pages 1138–1145, Halmstad, Sweden, June 2003. Springer Verlag.

[9] G. Loum, P. Provent, J. Lemoine, and E. Petit. A New Method for Texture Classification Based on Wavelet Transform. In *Third International Symposium on Time-Frequency and Time-Scale Analysis*, pages 29–32, June 1996.

[10] Stephane G. Mallat. A Theory for Multiresolution Signal Decomposition: The Wavelet Representation. *IEEE Trans. Pattern Analysis and Machine Intelligence*, 11(7):674–693, July 1989.

[11] Andrzej Materka and Michal Strzelecki. Texture Analysis Methods - A Review. Technical Report COST B11, University of Lodz, Institute of Electronics, Brussels, 1981.

[12] Michel Misiti, Georges Oppenheim, Jean-Michel Poggi, and Yves Misiti. *Wavelet Toolbox, User's Guid.* The Mathworks, July 2002.

[13] Miodrag Popović. Texture Analysis using 2D Wavelet Transform: Theory and Applications. In *4-th International Conference on Telecommunications in Modern Satellite, Cable, and Broadcasting Services, TELSIKS99*, pages 149–158, Niš, Yugoslavia, October 1999.

[14] R. Porter and N. Canagarajah. A Robust Automatic Clustering Scheme for Image Segmentation Using Wavelets. *IEEE Trans. Image Processing*, 5(4):662–665, 1996.

[15] R. Porter and N. Canagarajah. Robust Rotation Invariant Texture Classification. In *IEEE International Conference on Acoustics, Speech, and Signal Processing, ICASSP-97*, volume 4, pages 3157–3160, April 1997.

[16] R. Porter and N. Canagarajah. Robust Rotation-Invariant Texture Classification: Wavelet, Gabor Filter and GMRF Based Schemes. In *IEE Proc. Vision Image and Signal Processing*, volume 144, pages 180–188, June 1997.

[17] T. Randen and J.H. Husoy. Filtering for Texture Classification: A Comparative Study. *IEEE Trans. Pattern Analysis and Machine Intelligence*, 21(4):291–310, April 1999.

[18] P. Scheunders, S. Livens, G. Van de Wouwer, P. Vautrot, and D. Van Dyck. Wavelet-based Texture Analysis. *International Journal on Computer Science and Information Management*, 1(2):22–34, 199.

[19] Mona Sharma and Sameer Singh. Evaluation of Texture Methods for Image Analysis. In *7th Australian and New Zealand Intelligient Information Systems Conference*, pages 117–121, Perth, 2001.

[20] M. Tuceryan and A. K. Jain. Texture Analysis. In C.H. Chen, L. F. Pau, and P. S. P. Wang, editors, *Handbook of Pattern Recognition and Computer Vision*, pages 207–248. World Scientific Publishing Co., Singapore, 2 edition, 1998.

[21] IEEE Standard Glossary of Image Processing and Pattern Recognition Terminology, IEEE Std 610.4-1990, 1990.